Portable Life Support Subsystem Thermal Hydraulic Performance Analysis

Bruce Barnes, John Pinckney and Bruce Conger

Jacobs Engineering

Engineering and Science Contract Group

2224 Bay Area Blvd

Houston, Texas 77058

Ph: (281) 461-5871, email: bruce.barnes@escg.jacobs.com

ABSTRACT

This paper presents the current state of the thermal hydraulic modeling efforts being conducted for the Constellation Space Suit Element (CSSE) Portable Life Support Subsystem (PLSS). The goal of these efforts is to provide realistic simulations of the PLSS under various modes of operation. The PLSS thermal hydraulic model simulates the thermal, pressure, flow characteristics, and human thermal comfort related to the PLSS performance.

This paper presents modeling approaches and assumptions as well as component model descriptions. Results from the models are presented that show PLSS operations at steady-state and transient conditions. Finally, conclusions and recommendations are offered that summarize results, identify PLSS design weaknesses uncovered during review of the analysis results, and propose areas for improvement to increase model fidelity and accuracy.

1.0 Introduction

This paper describes the development of analytical and numerical methods based on known physical laws and well established correlations to predict the performance of the Constellation Space Suit Element (CSSE) Portable Life Support Subsystem (PLSS) baseline schematic and preliminary flexible PLSS design. Thermal Desktop™ (TD) thermal hydraulic model of the fluid flows within the PLSS and the Pressure Garment System (PGS) is documented in this report.

PLSS fluid performance is analyzed at the system level under anticipated ranges of operating conditions. To be successful, the analysis methods must predict temperatures, gas and liquid flow, heat flows, and gas species concentrations under time varying conditions that will be close to actual values to be experienced in the PLSS during service.

Validation of results will be established in experiments and measurements made during PLSS hardware manufacture, testing and service. This theoretical approach provides a cost-effective tool for the design process as a means of evaluating hardware design and material selection before manufacture. It predicts how individual components contribute to the total system.

This analysis precedes hardware development and is planned to be continued concurrently with the manufacturing and operation phases. It is planned to be a tool for evaluating future changes in the PLSS and PGS designs. The software chosen for this analysis is TD, which acts as a preprocessor for the Systems Improved Numerical Differencing Analyzer with Fluid Integrator (SINDA/FLUINT) distributed by C&R Technologies, Inc.

The scope of the effort includes the building and exercising of a PLSS system-level thermal hydraulic model using TD. Preliminary results of this model are presented and discussed in section 2.6. Being a system-level effort, individual components within the system are not modeled in detail.

The baseline CSSE PLSS schematic representation is shown in Figure 1: PLSS Schematic. For a detailed discussion of PLSS subsystem interrelations and device functions, see the PLSS Baseline Schematics and Internal Interfaces (Barnes, et al., 2009).

Although the schematic shown in Figure 1: PLSS Schematic covers multiple contingency modes as well as the normal Extravehicular Activity (EVA) mode only the normal EVA mode will be discussed here.

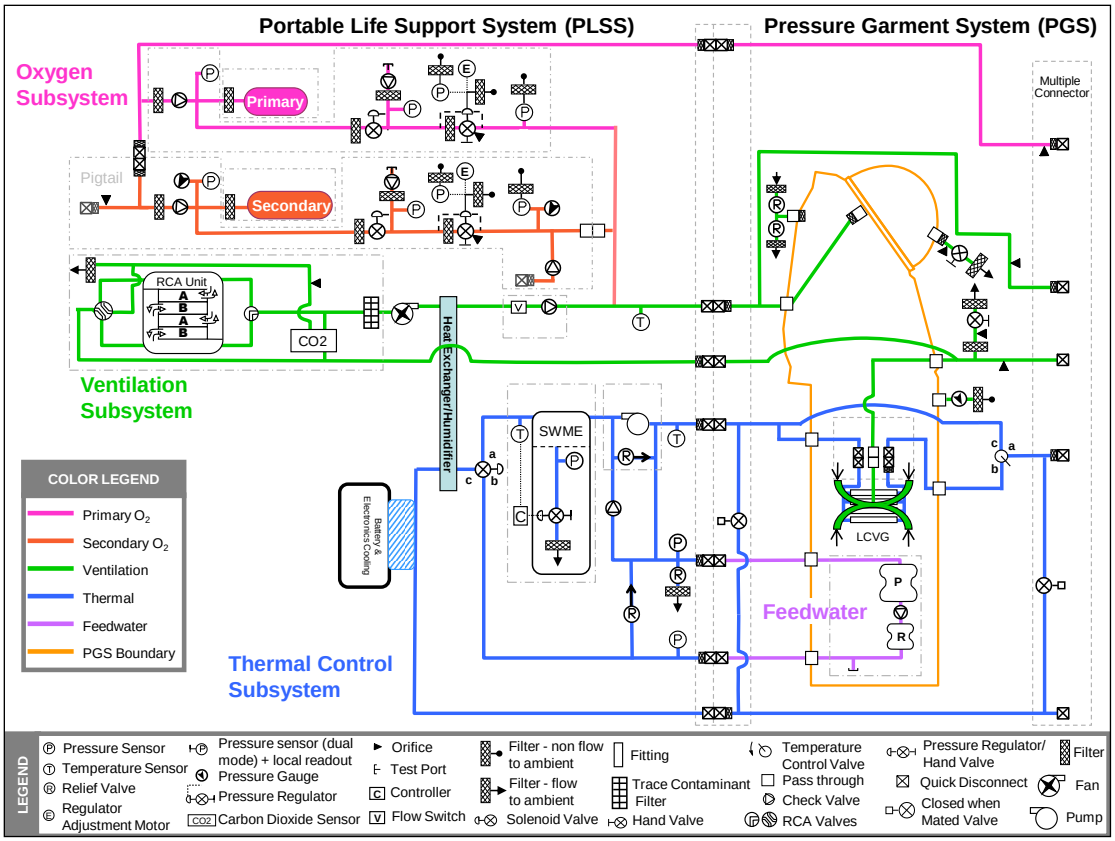

Figure 1: PLSS Schematic

2.0 Thermal Desktop Thermal Hydraulic Model

The TD thermal hydraulic model predicts temperatures, pressures, flow rates, and composition of the fluid systems throughout the CSSE PLSS.

2.1 Modeling Approach

The modeling software chosen to predict the PLSS thermal hydraulic performance is TD. TD generates an input file for SINDA/FLUINT. Only one-dimensional flow such as pipes and ducts can be analyzed. Frictional fluid losses from bends, surface roughness, orifices, and valves are calculated through known correlations. The frictional losses are converted into heating the fluid. Fluid kinetic energy is added to a fluid system by means of pumps and fans. Fans and pumps can be modeled as fan or pump elements with flow performance based on pressure versus flow curves. The effect of gravity on flow can also be included. The heat flow between solids and fluids is accomplished by conductors between fluid junctions and thermal nodes. Heat can be added directly to the fluid at any point.

TD provides a number of elements to model physical devices; these include tanks, tubes, orifices, bends, pressure regulators, check valves, control valves, pressure relief

valves (RV), as well as some special elements. Multi-species fluids (fluid mixtures that contain separate constituents such as a gas mixture containing carbon dioxide [CO_2], water [H_2O], and oxygen [O_2]) can also be modeled in TD; the partial pressures for each constituent are tracked in the case of gases or volume fraction in the case of liquids. Volumes within the system are modeled as tank elements. The tanks can hold fluid mass under pressure. The tanks can have rigid or flexible (compliant) walls.

TD can model gas-liquid phase changes. For example, if humid air cools to less than dew point, then a liquid fraction will be present and latent heat will be exchanged. TD also has special fluid nodes that have user-specified pressure and temperature as independent variables. These nodes function as infinite reservoirs for flow of fluid and energy.

TD allows the user to input custom code to model functions that can include control algorithms, constituent gas addition and removal (O_2, CO_2, and H_2O), and environmental heating effects. This capability was used extensively in the model.

A baseline TD schematic model was constructed by incorporating the proposed devices and subsystems of the PLSS. The TD schematic is shown in Figure 2: TD PLSS Schematic Model. The model is divided into two TD submodels: the vent loop (VL) and the Thermal loop (TL). The VL consists of O_2 subsystem and the Ventilation subsystem. These subsystems in the PLSS are involved in providing respiratory gas to the crewmember (CM). It consists of tubing, O_2 tanks, pressure regulators, Rapid Cycle Amine (RCA), fan, humidifier-heat exchanger, CO_2 sensor, pressure sensors, valves and restrictions. The TL provides active cooling or heating to the CM and PLSS components. The TL contains the H_2O pump, Spacesuit Water Membrane Evaporator (SWME), H_2O bladders, Liquid Cooling and Ventilation Garment (LCVG), tubing, valves, restrictions, and electronics. Heat and mass exchange between the subsystems is accomplished by conductors and SETFLOWs. A SETFLOW is a TD element that fixes the flow rate in fluid path to a constant value. It can be used to represent a very simple fan or pump, or it can be used to set the flow rate selectively for a constituent of the fluid stream such as CO_2, or H_2O.

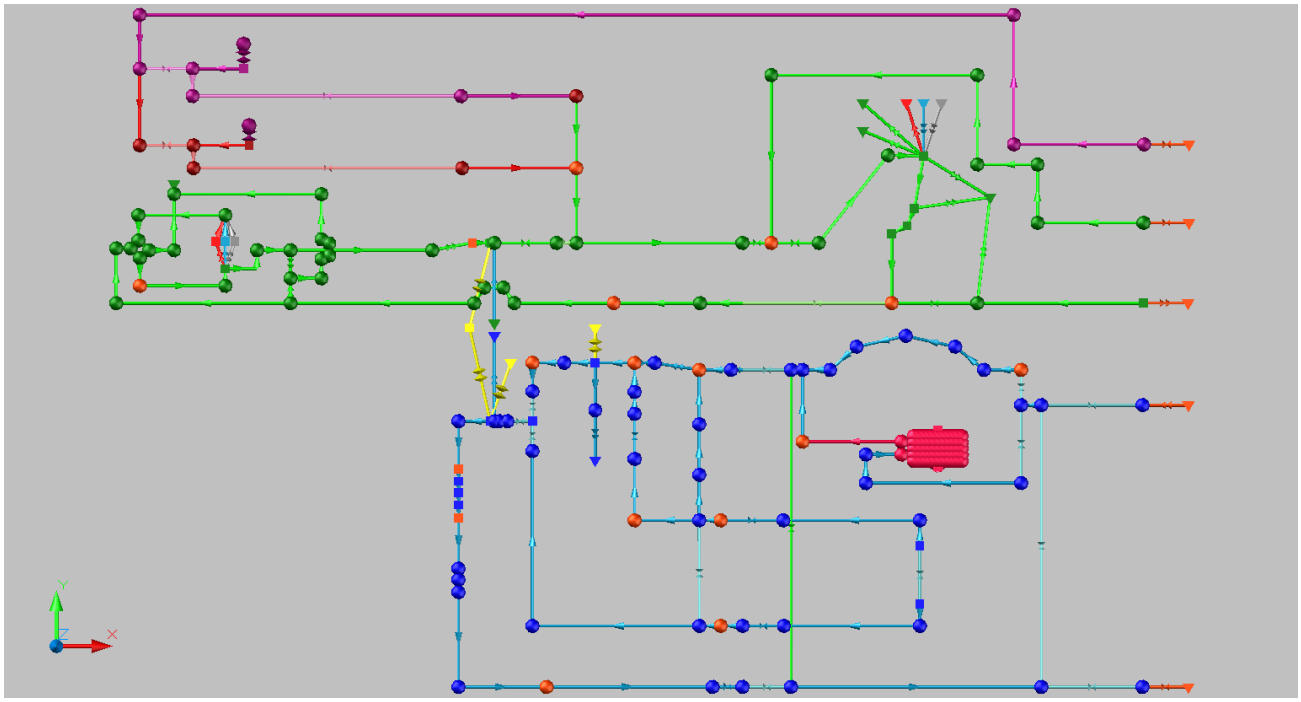

Figure 2: TD PLSS Schematic Model

The lines, circles, and squares represent tubing, fluid nodes, and tanks, respectively.

Mass rate contributions of CO_2 and H_2O from the CM are added to the VL. CM heat is added to the VL and the LCVG. Heat is removed from the TL by evaporation of H_2O by the SWME. H_2O is removed from the TL by a SETFLOW element connected to a boundary fluid node representing the vacuum.

Calculation of interaction between the CM and environment with the PLSS is simulated with the 41-Node Transient Metabolic Man Program (Bue, 1989) which is integrated into the TD model as is a SINDA model of one proposed PGS. The ambient environment and metabolic functions of the CM are treated as inputs to the model.

2.2 Modeling Assumptions and Techniques

The primary and secondary O_2 tank wall mass is modeled as a thermal node with a conductor to the O_2 mass to provide some thermal lag.

Tube modeling assumes no surface roughness. Pressure drop losses are computed by SINDA/FLUINT with standard correlations for smooth pipe (Cullimore, et al., 2006).

Flow changes in the tubes are reflected instantaneously. There is no delay in propagation of a physical variable from the inlet of a tube to the end. Currently the

volumes of the PLSS tubes are assumed to be zero and the fluid volumes for the entire PLSS are accounted for in tank nodes. Flow transients can be observed due to the presence of tanks and their associated volumes.

Metabolic rates modeled to date include a high rate (469 W), a moderate rate (293 W), and a low rate (117 W). Thermal environments modeled include the following cases:

- Hot case (121 °C [250 °F]) sink temperature
- Neutral case (21 °C [70 °F]) sink temperature
- Cold case (-198 °C [-325 °F]) sink temperature

2.3 Subsystem Model Descriptions

The descriptions of how the subsystems and components within the VL and TL are modeled are presented in the following subsections.

2.3.1 O_2 Subsystem

The O_2 subsystem provides O_2 to support CM metabolic makeup, suit leakage, RCA ullage losses, and CO_2 sensor sample losses. Suit pressure control is provided by the O_2 subsystem and emergency O_2 is provided by the secondary O_2 tank to support purge flow through the helmet that washes out CO_2 and is vented overboard. The subsystem contains a primary O_2 tank, a secondary O_2 tank, and regulators to control pressures within the VL and the suit.

2.3.1.1 O_2 Tanks

The main components of the O_2 subsystem are the primary and secondary tanks. The primary tank provides O_2 for the replenishment of losses in the ventilation subsystem due to metabolic consumption, RCA operation, and suit leakage. The secondary tank provides emergency back-up if the primary O_2 system fails or if the primary tanks empties.

The primary and secondary tanks are modeled in TD as tanks with volumes of 0.00284 m^3 (0.1001 ft^3) and 0.00450 m^3 (0.1591 ft^3), respectively, initially pressurized to 2.068×10^7 Pa_a (3,000 psia) at 20 °C (68 °F). The primary tank initially contains 0.77 kg (1.7 lb) of O_2 and the secondary tank contains 1.2 kg (2.7 lb) of O_2. The mass of the tank walls and its associated hardware (regulators, etc.) are modeled as a capacitive node with a tie to the O_2 volume. Addition of model representations for the tank walls and hardware will provide more accurate predictions of the O_2 temperature as the O_2 undergoes cooling during depressurization and heating during recharge.

2.3.1.2 O_2 Regulators

The pressure from the tanks is lowered to appropriate PGS pressures by pressure regulators. The pressure regulators for the tanks are set at 29,600 Pa_d (4.3 psid) and 24,800 Pa_d (3.6 psid) for the primary and secondary systems. The secondary tank begins to empty when the VL feed line pressure drops to the secondary regulator setting.

The O_2 pressure regulators are modeled as TD control valve elements with logic that varies the opening size to maintain target values for downstream pressure.

2.3.2 Ventilation Subsystem

The ventilation subsystem scrubs CO_2 and humidity from the ventilation circuit and thermally conditions the ventilation flow to be sent to the helmet. This subsystem includes a fan that provides the flow momentum throughout the circuit during normal Extravehicular Activity (EVA) Mode. It also includes the RCA unit that removes the metabolically generated CO_2 and humidity, the CO_2 sensor, the trace contaminant control unit (not currently modeled), and the humidifier-heat exchanger.

2.3.2.1 RCA

The RCA is represented by a pressure loss element and three connecting SETFLOW elements. The SETFLOW elements model the removal of gaseous constituents from the VL by the RCA. There is one SETFLOW element each for CO_2, H_2O, and O_2. The SETFLOW elements vent to a vacuum fluid node. CO_2 and H_2O removal rates are predicted using equations developed based on Hamilton Standard RCA test data. Ullage removal rate is based on volume loss per cycle per bed. Ullage loss is a result of opening the free volume in the unit to vacuum.

O_2 loss rate is increased due to RCA ullage and suit leakage.

Because the adsorption and desorption processes are reversible, the overall heat generation of the RCA unit is zero. However, the current model transfers 2 W of heat into the VL at the RCA due to ventilation flow through warm amine beds.

The RCA CO_2 and H_2O removal efficiency is dependent on the cycle time. The cycle time is currently fixed at 3 minutes (min). If desired, the cycle time could be controlled by using the CO_2 sensor with adjustments to control the CO_2 partial pressure.

The RCA pressure drop calculation assumes the current cylindrical RCA design. A pressure drop versus flow rate curve was developed by using pressure loss test data for the current cylindrical RCA design.

2.3.2.2 Fan

The fan is modeled as a SETFLOW element with a currently assumed constant mass flow of 7.8×10^{-4} kg/sec (6.2 lb/hr). Future work will include actual fan performance curves to determine flow rate.

Evaluating performance of candidate fans will involve using fan curves in the model. Fan curves have been implemented previously into the TD PLSS fluid model successfully, and after a fan is selected, the appropriate fan curve will be used.

2.3.2.3 Humidifier-Heat Exchanger

The humidifier-heat exchanger system used (HC-320/HX-526) performs humidity control and cools the ventilation gas. The current design is for a membrane evaporator similar in design to the SWME, but instead of evaporating into the vacuum, it evaporates into the ventilation stream. H_2O from the thermal loop is directed on one side of the membrane and the ventilation stream on the other side. Convective heat exchange occurs between the H_2O and the ventilation stream.

The humidifier-heat exchanger system is modeled as a SETFLOW element that removes H_2O from the TL and adds it to the VL. The VL has excessive H_2O removed by the RCA so H_2O is introduced by the humidifier-heat exchanger for CM comfort. Proportional control logic (control scheme that varies amount of H_2O added proportionally to how close the dew point is to the set point) is used to regulate the rate of H_2O added to maintain a dew point of 4.4 °C (40 °F) at the helmet (see Section 2.4.3.1,Humidity Control). The latent heat of vaporization is accounted for by heat removed from the TL.

The heat exchanger is modeled as a constant, overall heat transfer coefficient and area product (UA) between lumps in the TL and VL.

2.3.2.4 CO_2 Sensor

The CO_2 sensor is placed such that it can sense CO_2 at both the inlet and the outlet of the RCA. The RCA and the CO_2 sensor have a common exhaust to vacuum for the small stream of ventilation gas used for sampling. In the actual device, an internal switching valve alternately measures the CO_2 concentration in the gas stream before and after the RCA. Mass loss representing the sample stream flow to vacuum is accounted for by equal flows from each branch to vacuum.

2.3.2.5 Pressure Suit and CM

O_2 consumption, as well as CO_2 and H_2O production by the CM, are modeled with mass flows using SETFLOW elements into and out of the VL at the helmet. These mass flows are governed by the relationships from the 41-Node Transient Metabolic Man Program.

2.3.3 Thermal Subsystem

The thermal subsystem includes the components that control the temperature of the H_2O and also interfaces with the components that are thermally conditioned by the H_2O. The major goals of the thermal subsystem are to provide thermal comfort to the CM and maintain proper thermal conditions for the components within the PLSS. The major components include the SWME, the pump, and the H_2O bladders.

2.3.3.1 LCVG

The H_2O tube portion of the LCVG is modeled as a network of tubes with tank elements to account for the volume. Currently the tank walls are rigid. The overall pressure loss is comparable to LCVG for the Shuttle EMU.

The required amount of heat transfer between the LCVG and CM is defined by the 41-Node Transient Metabolic Man subroutines.

2.3.3.2 H_2O Bladders

Currently the model assumes that the primary and reserve H_2O bladders start with constant volumes.

The bladder compliance was calculated by using Shuttle EMU H_2O bladder test data (Falconi, 2004).

2.3.3.3 Temperature Control Valve

The temperature control valve (TCV), HV-512, is used by the CM to control his or her comfort. It allows control of diversion of constant temperature flow around the LCVG. The TCV is modeled by a control valve placed on each branch. Distribution of flow between the two branches is determined by relative opening of the two valves.

2.3.3.4 SWME

The SWME cools the TL by evaporation of H_2O through membrane material to vacuum. The PLSS team has recently down-selected to a hollow fiber SWME configuration (Bue 2010). The SWME performance in the TD model is currently modeled based on a

SWME technology using a thin, porous Teflon® membrane. The membrane is arranged in three concentric double-walled (coaxial) cylinders (see Figure 3: SWME End Cut (Concentric Cylinder Design)). The membrane is held in place by perforated plates and H_2O flows down the cylinder between the membrane walls. Surfaces exterior to the annuli are exposed to the vacuum through the exhaust valve.

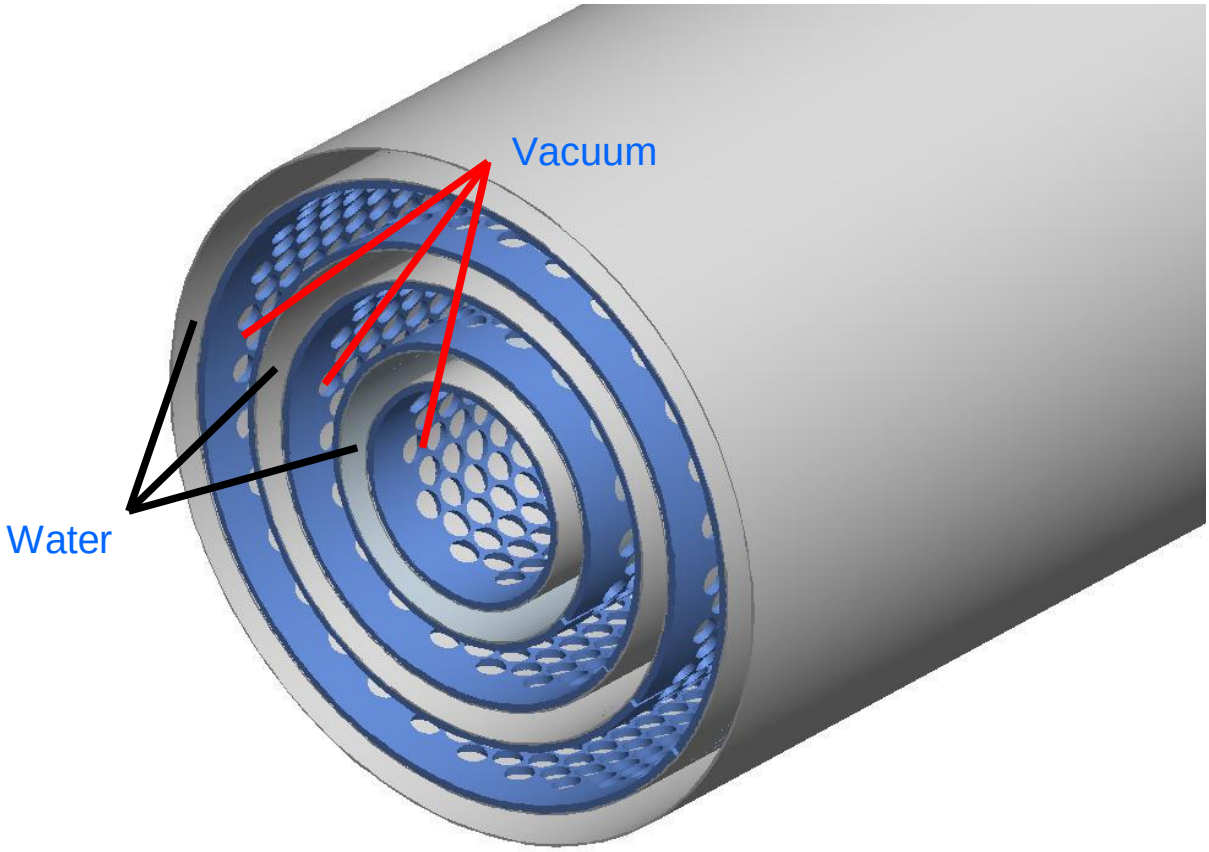

Figure 3: SWME End Cut (Concentric Cylinder Design)

The rate of evaporation is proportional to the difference in the gaseous H_2O pressure across the membrane. The H_2O pressure inside the membrane is given by the saturation pressure of H_2O, and H_2O pressure outside the membrane is controlled by the SWME exhaust valve. Equation 1 governs the process (Ungar and Thomas, 2001).

Equation 1: SWME Heat Removal

$$q'' = 0.83\frac{d}{3}\sqrt{\frac{8}{\pi R T_{int\,erface}}}\frac{[p_{sat}(T_{int\,erface}) - p_{out}]h_{fg}}{L}$$

Where:

d	membrane pore size (0.10μ)	(m)
h_{fg}	heat of vaporization for H_2O	(kJ.kg)
L	thickness of the membrane (25 μ)	(m)
q”	energy flux at the liquid/vapor interface	(W/m2)
p_{sat}	H_2O saturation pressure	(Pa)
p_{out}	pressure external to the membrane	(Pa)
R	gas constant for H_2O	(kJ/kg K)
$T_{interface}$	temperature of H_2O at liquid/vapor interface	K

The heat removal rate is proportional to the difference between the H_2O saturation pressure and the external pressure. The saturation pressure of H_2O at the operating temperatures of the SWME is less than the operating H_2O pressure of the TL; this implies that the H_2O evaporates only at the pore locations.

P_{sat} has strong dependence on T (see Equation 2) in the T range of operation. The relative change in P_{sat} is about 6 percent.

Equation 2: H_2O Saturation Pressure at SWME

$$\frac{\frac{d}{dT}P_{sat}(T)}{P_{sat}(T)} = \frac{6\% - 7\%}{K}$$

As the H_2O traverses the SWME, it cools, lowering P_{sat} and the cooling capacity per unit area.

A steady-state thermal model was constructed independently to predict SWME performance (Vogel, 2008). The model calculated local H_2O T and corresponding heat flux. The annular flow areas that vent to vacuum are sufficiently large that there is no significant pressure drop within the SWME even at maximum cooling rates. Equation 3 is an equation curve fit to the independent model results that predicts the minimum membrane temperature of the SWME, which drives the maximum SWME cooling rate. This equation is used in the model.

Equation 3: SWME Maximum Cooling Rates

$$Tif_{max} = -0.0050526 \cdot Tin\text{^}2 + 3.58055 \cdot Tin + (-330.596)$$

Where Tif_{max} is the interface temperature (K) corresponding to maximum SWME heat flow capability and Tin is the temperature (K) of fluid entering SWME.

The SWME is represented with a tank and a SETFLOW element. H_2O loss through the SWME is modeled as a variable SETFLOW. The removal rate is calculated from cooling rates. The cooling rate is determined by a proportional control logic that adjusts cooling to meet LCVG target temperatures.

2.3.3.5 Pump

The pump is modeled as a SETFLOW element at 91 kg/hr (200 lb/hr). Future enhancement will include a pump performance curve. The model currently assumes that the pump adds 10 W to the TL.

2.4 Heat and Mass Accounting

The thermal and mass interactions between the CM and the PLSS are complex. The model includes the 41-Node Transient Metabolic Man Program to predict these interactions.

The heat loads of the various PLSS components are presented in the following section and will be updated as information becomes available on actual component selection and design.

2.4.1 Heat Balance

Heat is added to the PLSS by powered components, the CM, and the environment. The environmental heating is added directly to the TL at the outlet of the LCVG and is based on an incorporated SINDA model of a space suit.

Table 1: Component Heat Loads shows the model assumption for the amount of heat added by powered components.

Table 1: Component Heat Loads

H_2O Loop	**Heat**
Pump	10 W
Electronics/Battery	41 W
Vent Loop	**Heat**
Fan	7 W
RCA*	2 W

*RCA adds 2 W to the ventilation stream even though the RCA process produces no net heat on average. The ventilation flow passes through the exothermic bed and is warmed, but an equal amount of heat is added to the desorbing bed from its surroundings. The 2 W value also includes the power required to operate the RCA cycling valve.

2.4.2 Fluid Energy Loss

Energy is lost in a fluid system due to friction between fluid elements and system fixture hardware (such as pipe walls, connectors, and valves) and viscous forces between fluid elements. Currently, the model does not incorporate friction losses with hardware. Losses due to this will be added in future refinements to the model.

2.4.3 Mass Balance

H_2O, CO_2, and O_2 are removed from the VL by the operation of the RCA and suit leakage.

Mass is removed from the VL by the RCA, CO_2 sensor, and suit leakage. Mass is added to the VL by the O_2 tanks and the humidifier. The CM removes O_2 from the VL and adds H_2O and CO_2 to the VL.

2.4.3.1 Humidity Control

To control humidity, the dew point is controlled. The maximum dew point is estimated to be 4.4°C (40°F) to prevent visor fogging within the helmet. This is a goal in the model. Humidity is added to the VL by the humidifier. In general, the VL atmosphere will be too dry (causing dryness issues in the oral-nasal areas of the astronaut) due to excessive H_2O scrubbing by the RCA. The dew point is calculated by inverting the Arden-Buck equation (see Equation 4) for saturation pressure of H_2O:

Equation 4: Saturation Pressure of H_2O

$$Psat = 611.21 * e^{\frac{\left(18.678 - \frac{T}{234.54}\right) * T}{\left(257.17 + T\right)}}$$

2.5 Results and Discussion

Steady-state and transient results for certain parameters under chosen conditions are presented and discussed in the following subsections. Steady-state values represent a snapshot at a point in time during a transient simulation when conditions have leveled out and are not changing with time. The parameters and conditions presented are selected to give a broad representation of the model's capabilities and preliminary results. As the PLSS design matures and testing is performed, the predictions from this model will continue to improve in fidelity and accuracy. Also, TD allows results to be presented in various units independent of the units used for model creation. Metric units are presented for the results that follow.

2.5.1 Steady-State Results

Steady-state results are shown schematically for the normal EVA cases under the following conditions:

- High metabolic rate in the hot environment
- Moderate metabolic rate in the neutral environment
- Low metabolic rate in the cold environment

See Section 2.2, Modeling Assumptions and Techniques, for definitions of the environments and metabolic rates. The TD thermal hydraulic model has been run as a transient in all cases; however, the temperatures and flow rates stabilize after a certain duration. These stabilized conditions are the results reported in this study.

2.5.1.1 Normal EVA Results

Normal EVA results for all metabolic rates and environments are shown in tabular format in Appendix A. Figure 4: Normal EVA - Hot Environment – High Metabolic Rate, Figure 5: Normal EVA - Neutral Environment – Moderate Metabolic Rate, and Figure 6: Normal EVA - Cold Environment – Low Metabolic Rate, present results from three of these normal EVA cases. Temperatures at nodes (TD lumps) are color-coded, labeled at selected nodes, and correspond to the color bar on the bottom of the figure. Flow rates in the paths are color-coded, labeled at selected paths, and correspond to the color bar on the right side of the figure for the TL and on the left for the VL. The use of the two Flow rate color bars to due to the large difference in flow rates between the two subsystems.

For the hot, high metabolic rate case (Figure 4), almost no flow is diverted around the CM to provide the necessary thermal comfort to the CM via the LCVG. The temperature of the VL ranges from 17 ˚C to 51 ˚C (62 ˚F to 124 ˚F), being cooled by the humidifier-heat exchanger and peaking in temperature due to heating from the fan motor. The fan heat is transferred to the VL. The O_2 temperature inlet to the VL is predicted to be -10 ˚C (14 ˚F) due to expansion cooling in the O_2 tank.

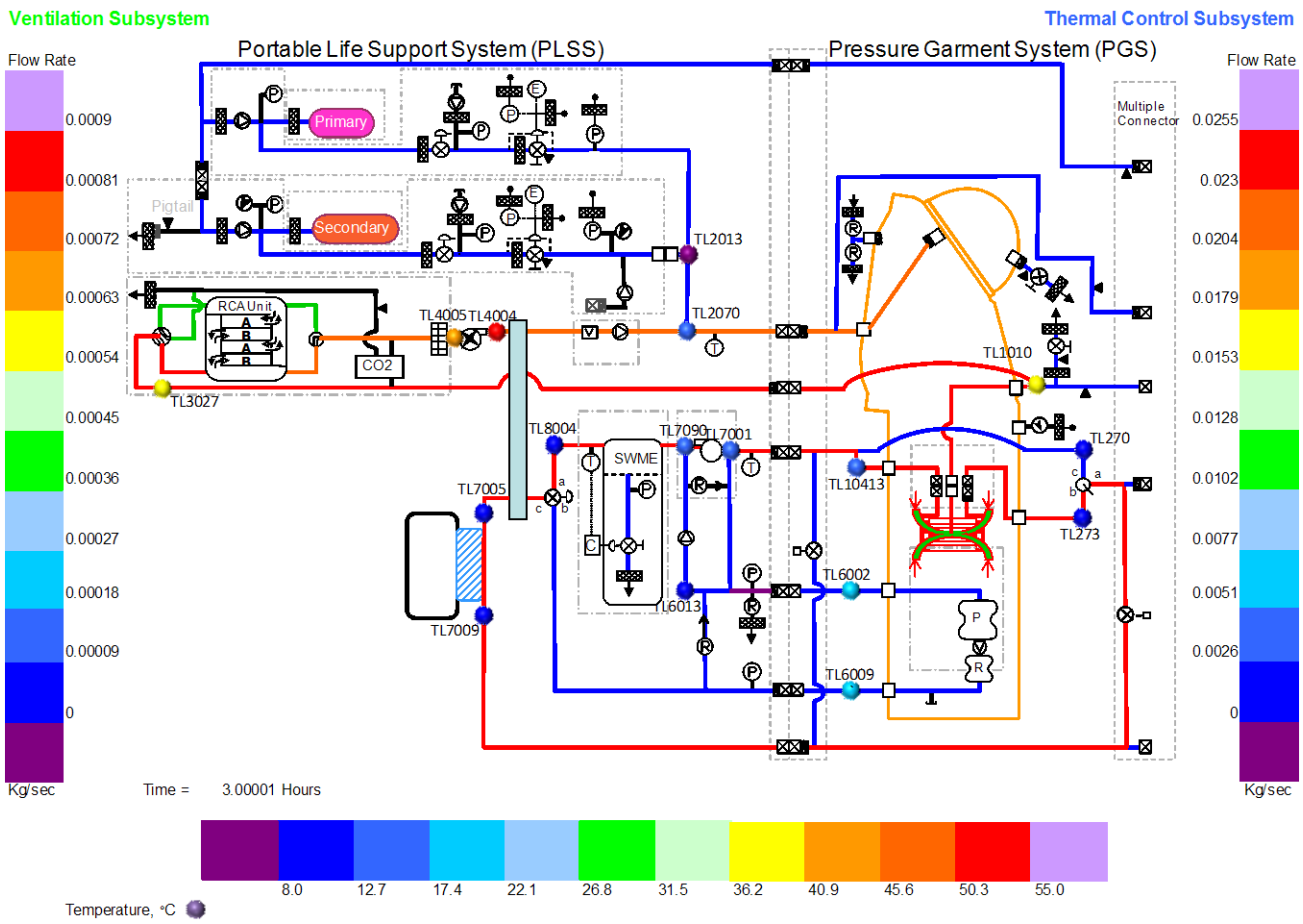

Figure 4: Normal EVA - Hot Environment – High Metabolic Rate

Figure 5 shows the CM bypass receiving more flow than in the hot, high metabolic case. This flow rate reflects the increased LCVG cooling requirement to the CM relative to the hot, high metabolic rate case. The O_2 temperature inlet to the VL is predicted to be -6 ˚C (31 ˚F) due to expansion cooling in the O_2 tank. This value is not as cool as the hot, high metabolic rate case because the O_2 flow rate is lower, due to the reduced metabolic requirement, and thus expansion cooling within the O_2 tank is less.

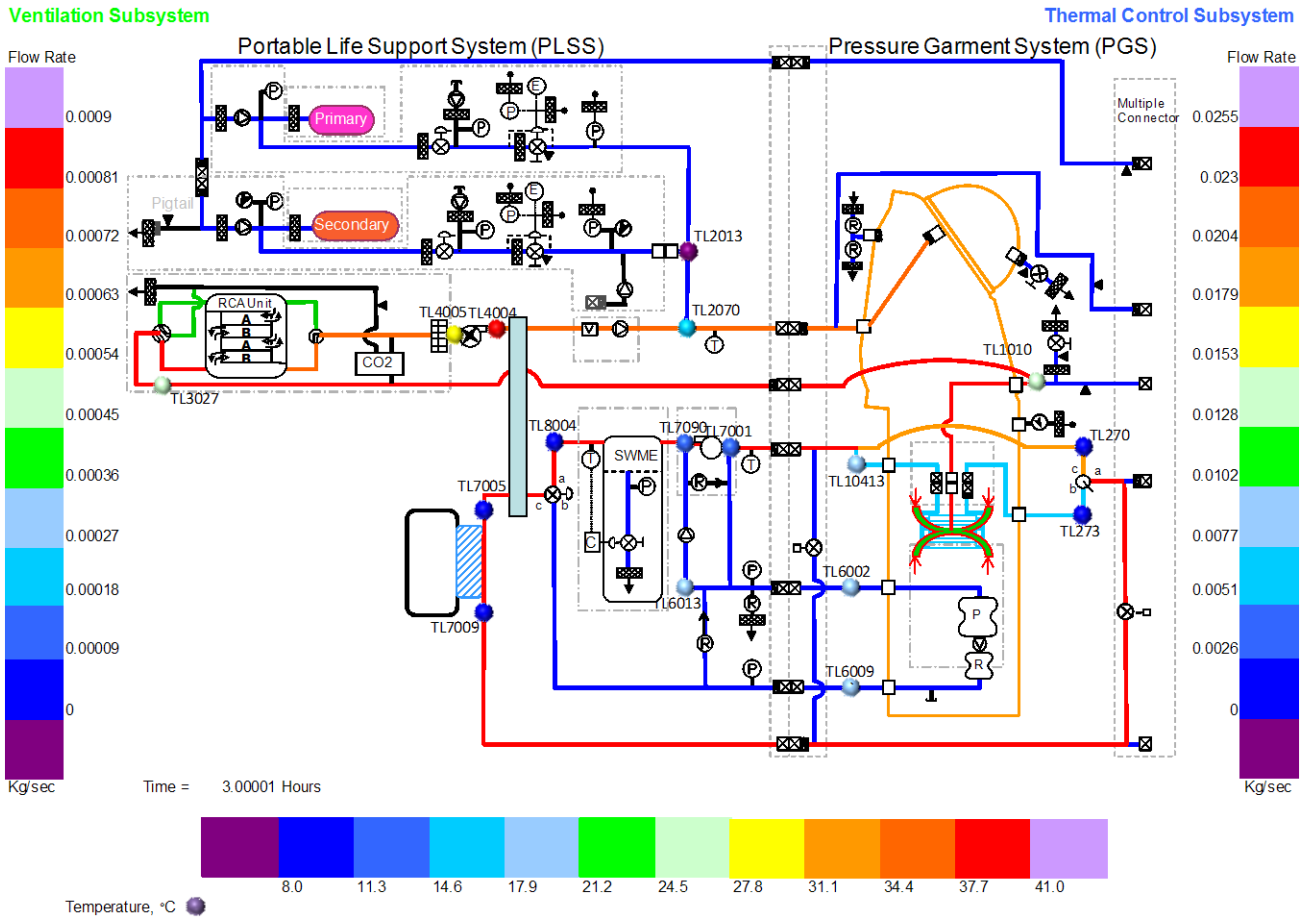

Figure 5: Normal EVA - Neutral Environment – Moderate Metabolic Rate

For the cold environment, low metabolic rate case, the flow rate to the CM is at a minimum to keep the CM warm. The VL provides a small amount of sensible heating to the CM in this simulation. The O_2 temperature inlet to the VL is predicted to be 9 ˚C (48 ˚F) due to expansion cooling in the O_2 tank. This value is not as cool as the previous cases because the O_2 flow rate is lower, due to the reduced metabolic requirement, and thus expansion cooling within the O_2 tank is less.

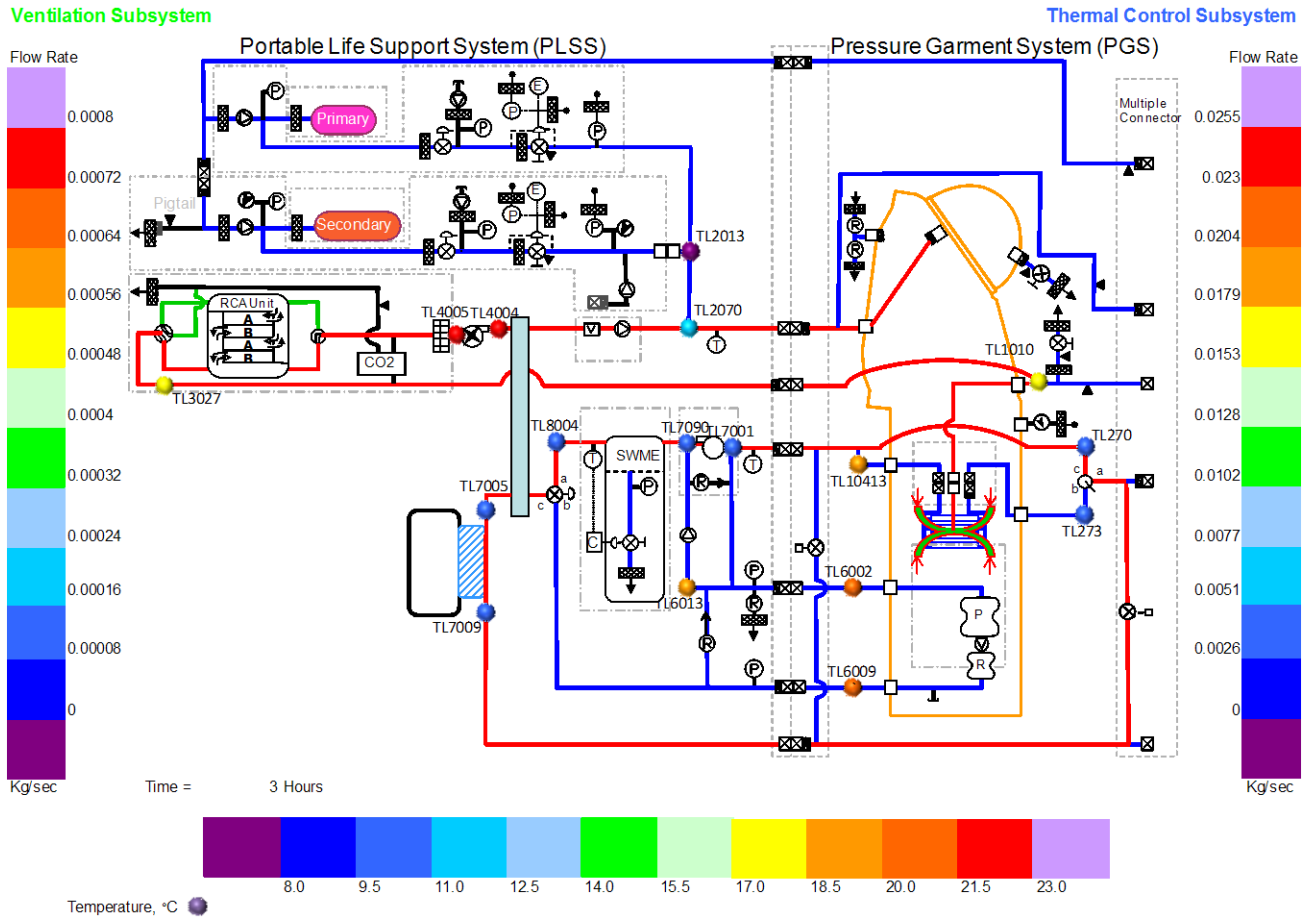

Figure 6: Normal EVA - Cold Environment – Low Metabolic Rate

The CO_2 and H_2O concentrations during a normal EVA in a hot environment at the high metabolic rate are presented in Figure 7: Normal EVA CO_2 Partial Pressure & Dew Point Distribution. For this example the RCA beds are cycled when the RCA outlet CO_2 concentration reaches 533 Pa (4 mmHg). The dew point coming out of the RCA is predicted to be -8 ˚C (18 ˚F), which is too dry for the CM. The humidity level is controlled to the desired minimum dew point of 4.4 ˚C (40 ˚F) at the humidifier. Humidity is added to the VL in the LCVG due to respiratory latent, and perspiration from the CM and the dew point at the exit of the LCVG is elevated to 15 ˚C for this case.

The average CO_2 partial pressure is predicted to be close to 1,666 Pa (12.5 mmHg) at the outlet of the suit at this high metabolic rate condition. The RCA performance algorithm predicts the outlet of the RCA CO_2 partial pressure to be an average of approximately 700 Pa (5.25 mmHg). The ventilation flow rate into the helmet was controlled to $1.1x10^{-3}$ kg/sec (6.0 ACFM) to meet this CO_2 requirement.

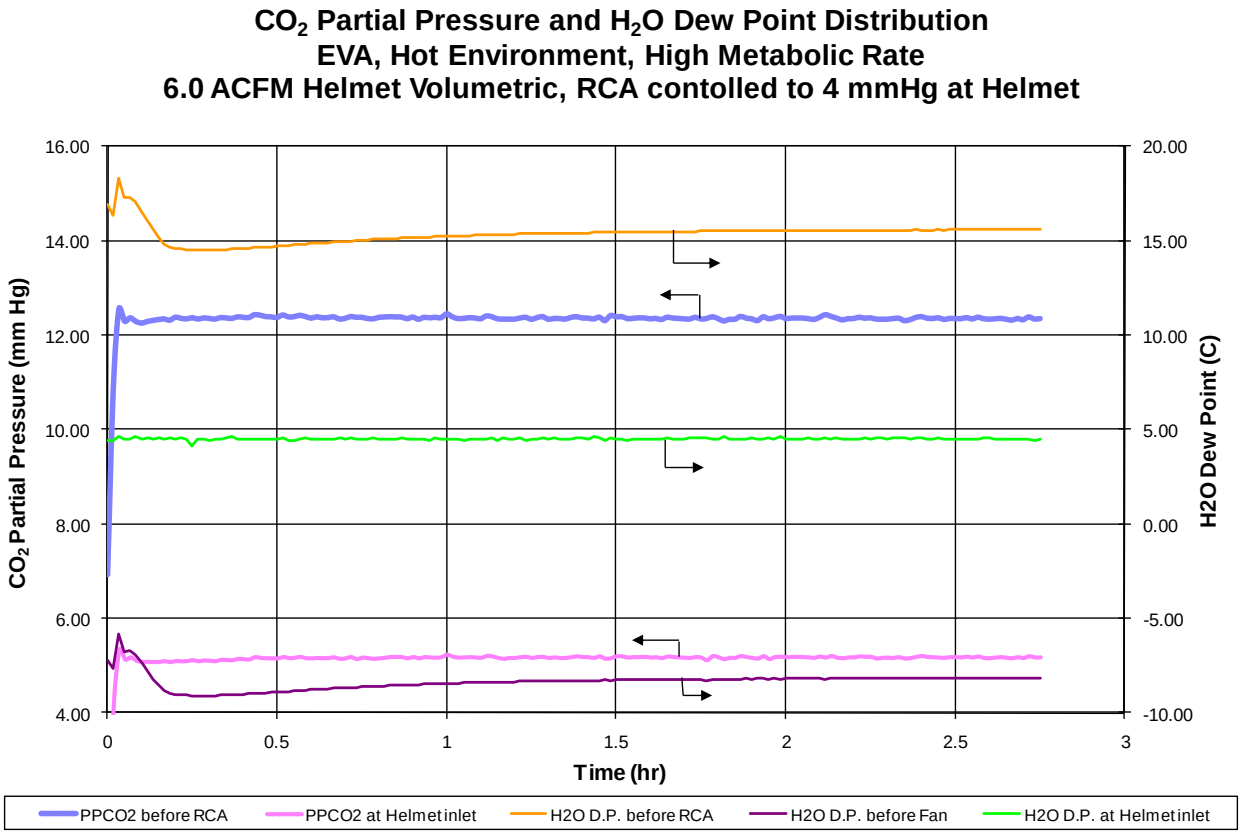

Figure 7: Normal EVA CO_2 Partial Pressure & Dew Point Distribution

Table 2: SWME Cooling Loads during Normal EVA Mode shows the cooling requirements that the SWME must meet to cool the entire suit during normal EVA Mode. Cooling loads are shown at the three metabolic rates and three environments analyzed. The hot environment with the high metabolic rate shows the highest cooling requirement, as expected, and is predicted by the model to be approximately 631 W. The low metabolic cold case shows the other extreme and predicts that the SWME needs to provide approximately 30 W of cooling.

Table 2: SWME Cooling Loads during Normal EVA Mode

Thermal Environment	***SWME Cooling Load (W)***		
	Low Metabolic Rate	*Moderate Metabolic Rate*	*Hi Metabolic Rate*
Hot	*-313*	*-482*	*-666*
Nom	*-156*	*-273*	*-454*
Cold	*-71*	*-185*	*-363*

2.5.2 Transient Results

Overall PLSS level transient results are discussed in the subsections below followed by ventilation subsystem results, O_2 subsystem results, and finally, thermal subsystem results.

2.5.2.1 PLSS Level Transient Results

Figure 8: Response to Metabolic Rate Changes shows the response of the system to the recommended EVA metabolic profile. The amount of bypass flow is based on providing thermal comfort to the CM at various metabolic rates. The chart indicates the lack of a healthy control scheme.

Currently a PID control algorithm is used causing the swings to achieve the bypass flow necessary to achieve CM comfort. However, the current operating assumption is that the CM will control the bypass flow directly and each individual CM will have varying algorithms in adjusting the bypass flow.

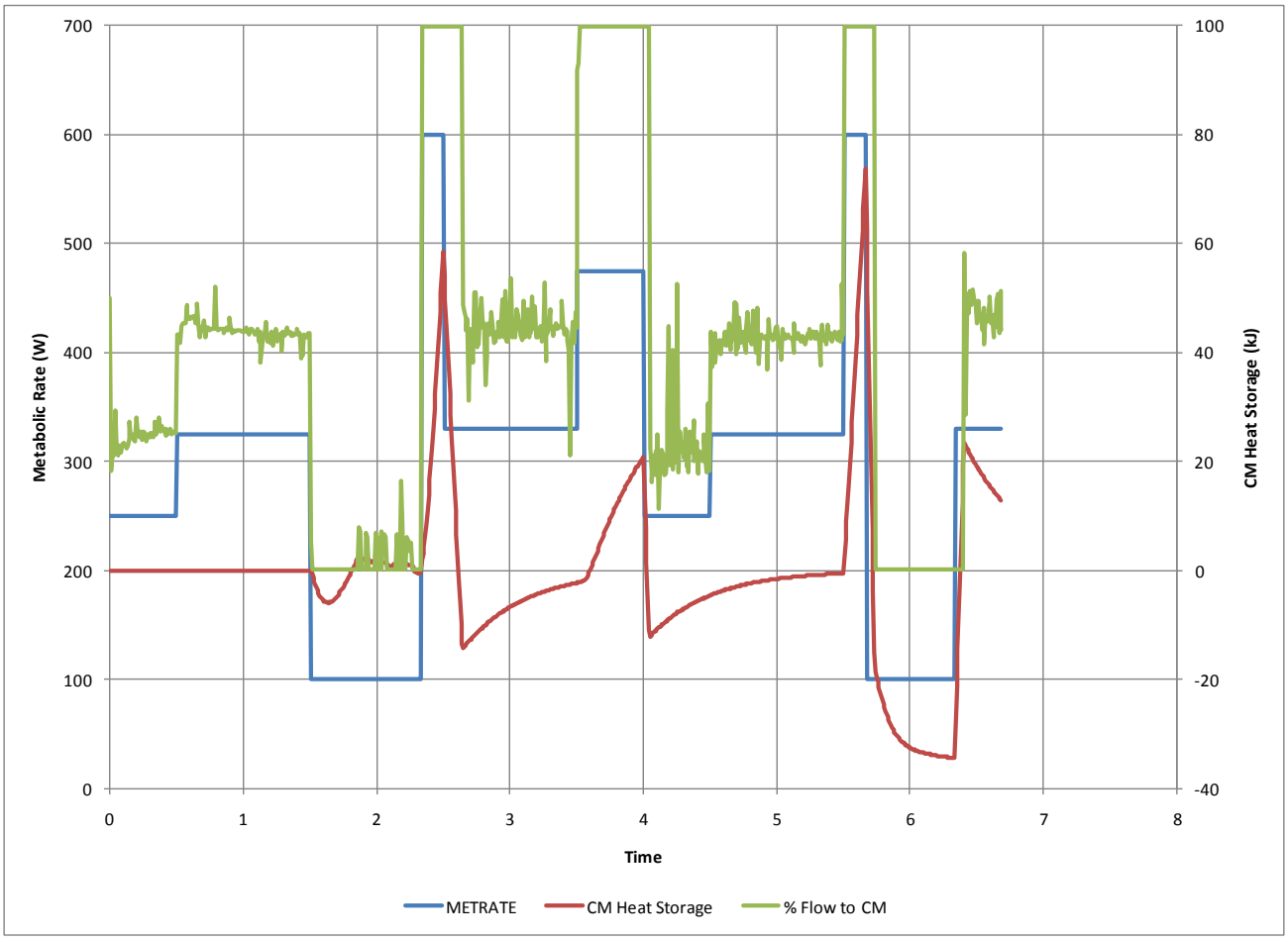

Figure 8: Response to Metabolic Rate Changes

2.5.2.2 O_2 Subsystem Transient Results

Figure 9: Recharge Response of O_2 Tanks presents the condition of the O_2 in its tanks during a recharge. The temperature response indicates significant warming due to compression heating. As the temperature of the O_2 decreases, the density of the O_2 increases and additional mass is added to the tanks. This recharge simulation assumes a constant 2.068×10^7 Pa_a (3,000 psia) source pressure at the umbilical inlet.

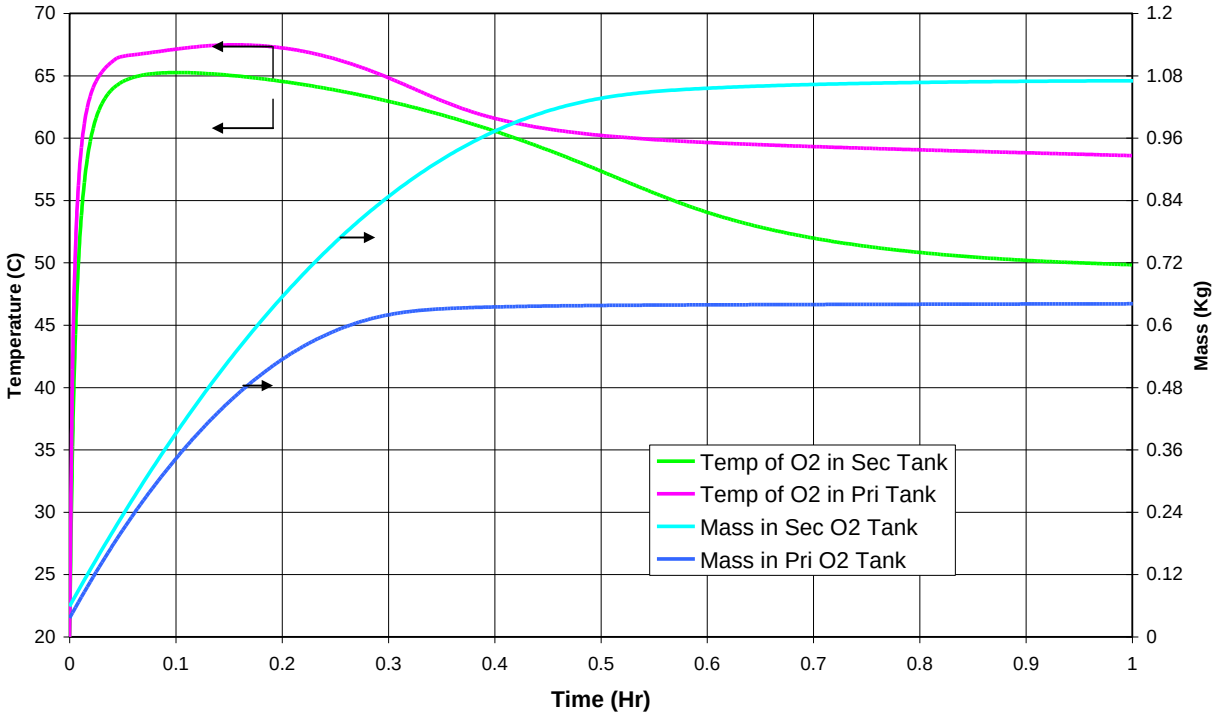

Figure 9: Recharge Response of O_2 Tanks

Figure 10: Primary to Secondary O_2 Transition Flow Rates, demonstrates the simulated transition from primary to secondary O_2. The flow rate drops to 0 kg/sec (0 lb/hr) during this transition. The primary O_2 regulator controls to 29,600 Pa_d (4.3 psid) and the secondary O_2 regulator 24,800 Pa_d (3.6 psid). When the primary O_2 tank is essentially empty, flow is stopped. The secondary flow is initiated when the pressure in the VL drops to 24,800 Pa_d (3.6 psid), thus accounting for the no-flow period. The suit O_2 pressure profile in Figure 12: H_2O Bladder Transition is an example of pressure changes during a transition from primary to secondary O_2.

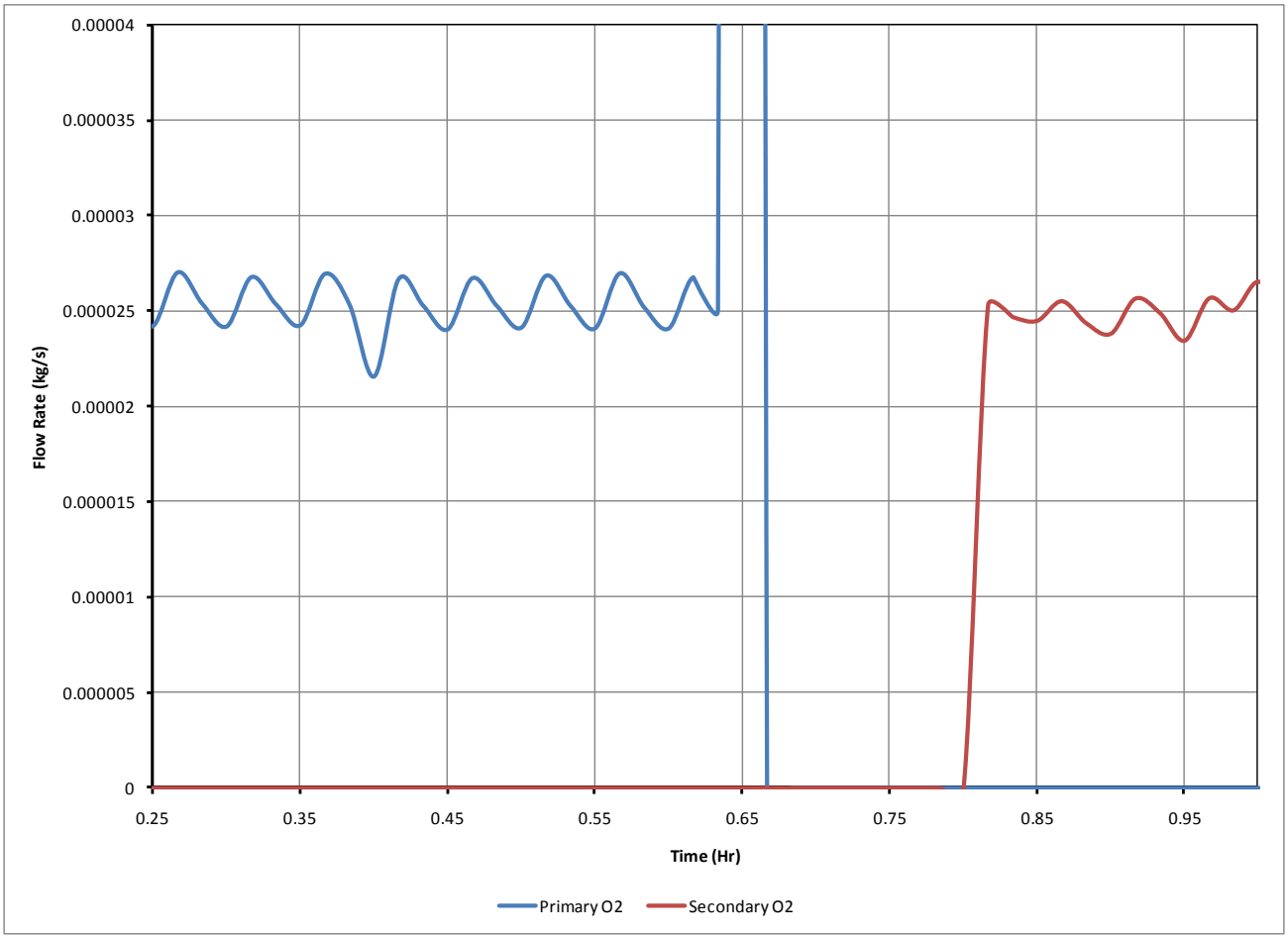

Figure 10: Primary to Secondary O_2 Transition Flow Rates

2.5.2.3 Thermal Subsystem Transient Results

Figure 11: SWME Transient Temperature Response shows SWME performance in response to a significant metabolic change from a low rate (117 W) to a high rate (469 W) and back down to the low rate during normal EVA Mode in a hot environment. The SWME heat removal rate is plotted along with the heat storage of the CM. This indicates a control problem which will be investigated in the future.

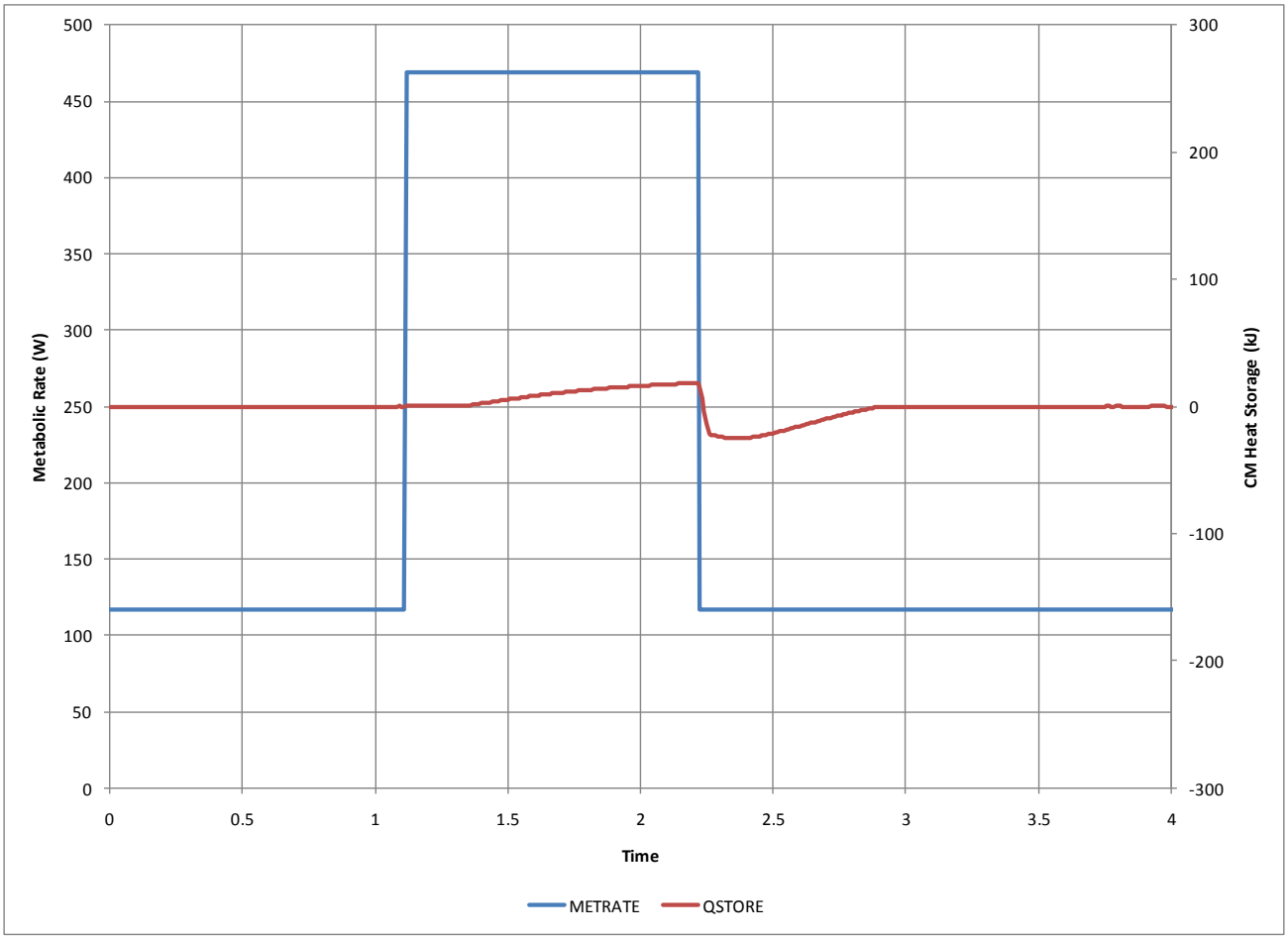

Figure 11: SWME Transient Temperature Response

Figure 12 : H_2O Bladder Transition depicts H_2O bladder and suit ventilation pressures during normal EVA Mode in a cold environment at a high metabolic rate. In this case, the primary O_2 tank is depleted, which is indicated by the first transition from 30,000 Pa_d (4.3 psid) to 25,000 Pa_d (3.6 psid). Pressure spikes at the start of the Primary to Secondary O_2 tanks, this is because when the Primary tank drops to below 50 psia the pressure regulator opens fully. Just before the 3-hour mark of this simulation, the primary H_2O bladder begins to run dry and pressure difference between the two bladders drops to 10,000 Pa_d (1.5 psid). When this drop occurs, H_2O flows from the reserve bladder via a relief valve between the two bladder outputs (see Figure 1) and maintains the pressure of the primary bladder at 10,000 Pa_d (1.5 psid) below the pressure of the reserve bladder. Pressure of the TL and the primary bladder is maintained at 10,000 Pa_d (1.5 psid) because RV-524 is set to trigger at a delta pressure of 15,000 Pa_d (2.2 psid). After the reserve bladder runs dry, both the primary and reserve bladder pressures drop rapidly.

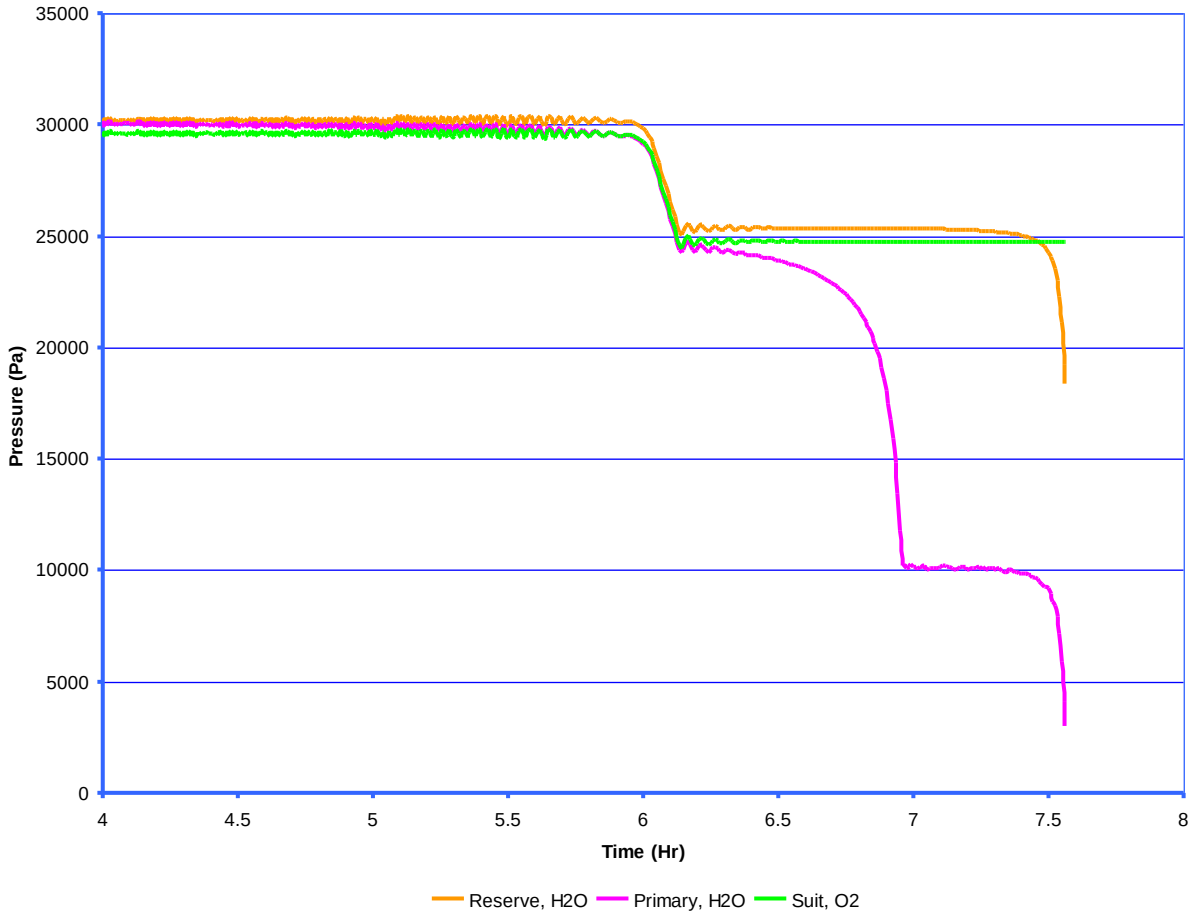

Figure 12: H_2O Bladder Transition

Figure 13: Bladder Flow during Transition shows the model prediction when the primary H_2O bladder is depleted and switches over to use the reserve bladder for normal EVA in a hot environment at a high metabolic rate. When the primary bladder runs dry, the reserve bladder not only flows into the TL, but also refills the primary bladder to some degree in this simulation.

When the primary bladder has been depleted, the relief valve activates and flows H_2O from the reserve bladder until the TL pressure equalizes with the reserve tank pressure. H_2O usage by the SWME then draws the TL pressure down and the relief valve again activates to equalize pressures. This pressure drop and equalization cycle explains the flow pulsations seen through the relief valve.

The results in Figure 12 and Figure 13 are dependent on the actual bladder hardware and relief valve performance characteristics. As these designs mature and relevant data become available, the associated characteristics will be revised in the model and the results will be updated.

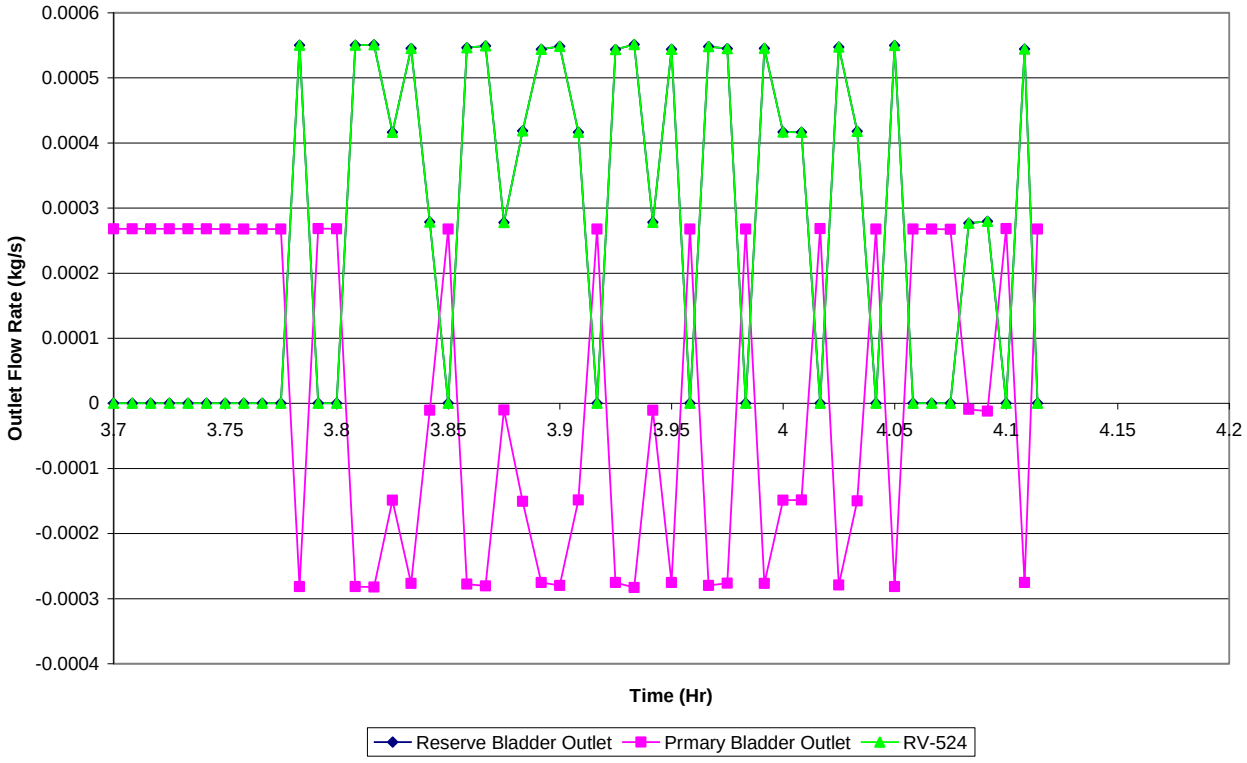

Figure 13: Bladder Flow during Transition

3.0 Conclusions and Recommendations

The PLSS thermal hydraulic analysis results have been discussed and reviewed. The results are preliminary, but trends appear to be reasonable for predicting the PLSS performance under varying environmental loads and metabolic rates. Verification and

enhancement of the models will be performed as the PLSS design matures and testing of prototype hardware is performed. The simulation results provide some insight into how components perform together when integrated into the PLSS. These simulations and predictions should help eliminate some of the surprises associated with hardware development and testing. These capabilities will also be useful in predicting performance during lunar surface operations that will be difficult to test on Earth with limited resources.

The following are recommendations for enhancements to the thermal hydraulic model:

- Evaluate condensation effects and the quantity of H_2O vapor that the suit, LCVG, and ventilation loop can carry.
- Figure 8 and Figure 11 demonstrate the need for better CM comfort control. A study of various thermal loop control schemes is to be instigated.
- Recently the TD thermal hydraulic model with Metman has been merged with the TD physical geometry model. This merged model should be verified and documented.
- Integrated Testing Analysis with Pretest planning & predictions, Post test analysis and correlation activities.
- Update and correlate component models as component design and prototype test results become available; increase modeling detail and fidelity for individual PLSS components.
- Update SWME modeling to represent the hollow fiber SWME technology performance.
- Update electronics and battery heat loads as required.
- Update and add connector and fitting pressure drop characteristics.

Upon incorporation of the recommended upgrades, the thermal hydraulic model will provide more accurate predictions for the PLSS that should provide valuable guidance to the CSSE PLSS design and development program.

The following are recommendations for future investigations to be performed with the model:

- Helmet CO_2 washout efficiency vs. RCA sizing trade study.
- Evaluate Cold O_2 purge issue with updated regulator models.
- Time to thermal comfort limits during failures evaluation.
- Evaluate ejector emergency oxygen capability.
- Expanded Filter Study.

- Replace Metman with higher fidelity Wissler human thermal model in PLSS Integrated Thermal Desktop model.
- Metabolic profile evaluation for various potential NASA missions.
- CO_2 sensor study.
- Ventilation loop flow switch vs. flow meter trade.
- PLSS schematic suit port compatibility evaluation.
- GORTEX bladder evaluation (water permeability investigation).
- TCCS location trade study.

References

Ames, Brian and John Iovine. “LESC-28227/CTSD-0638, Life Support Options Performance Program Version II.” Houston: Lockheed Engineering and Sciences Company, April 1990.

Bue, Grant. “LESC-27578/CTSD-0425, 41-Node Transient Metabolic Man Program.” Houston: Lockheed Engineering and Sciences Company, October 1989.

Bue, Grant and Luis A. Trevino. “Hollow Fiber Spacesuit Water Membrane Evaporator Development and Testing for Advanced Spacesuits.” Houston: NASA, JSC, October 1989.

Barnes, Bruce, Bruce Conger, Greg Leavitt, and Jennifer Wells. “JSC–65563/CTSD-CX-5117, PLSS Baseline Schematics and Internal Interfaces.” Rev. B. Houston: NASA, JSC, August 2009.

Cullimore, B. A., S. G. Ring, D. A. Johnson. “User’s Manual SINDA/FLUINT General Purpose Thermal/Fluid Network Analyzer Version 5.0.” Patch 3i, Littleton, Colorado: C&R Technologies, Inc., October 2006.

Falconi, Eric. “TPS #1K0420073, Perform Modified Feedwater Pressure Bingo Testing on SEMU 3003 in EMU Lab.” Houston: NASA, JSC, October 2004.

Thomas, Gretchen, Scott Schneider, Maria Keilich, and Bruce Conger. “Crewmember/Extravehicular Mobility Unit Thermal Interactions Affecting Cooling Preferences and Metabolic Water Removal.” Houston: NASA, JSC, International Conference on Environmental Systems #951637, July 1995.

Ungar, Eugene and Gretchen Thomas. “Design and Testing of a Spacesuit Water Membrane Evaporator.” Houston: NASA, JSC, Proceedings of 2001 National Heat Transfer Conference, June 2001.

Vogel, Matt R., Luis A. Trevino, Keith Peterson, Felipe Zapata III, and Paul Dillon. “Spacesuit Water Membrane Evaporator Development for Lunar Missions.” Houston: NASA, JSC, International Conference on Environmental Systems # 2008-01-2114, July 2008.